Acta Crystallographica Section D
Biological Crystallography
ISSN 0907-4449

Dehydration leads to a phase transition in monoclinic factor XIII crystals

Manfred S. Weiss* and Rolf Hilgenfeld

Institute of Molecular Biotechnology, Department of Structural Biology and Crystallography, PO Box 100813, D-07708 Jena, Germany

Correspondence e-mail: msweiss@imb-jena.de

Received 30 June 1999
Accepted 5 August 1999

Dedicated to Georg E. Schulz on the occasion of his 60th birthday.

Monoclinic factor XIII crystals have been transferred to a solution containing increasing amounts of the precipitant PEG 6000. At a concentration of about 36%(*w*/*v*) PEG 6000, a phase transition was observed. The space group of the crystals was preserved on the transition, but half of the 2_1 screw axes were lost, which meant that the unit-cell volume and the content of the asymmetric unit were doubled. The structure of factor XIII in the new crystal form was solved by molecular replacement. About 80% of the changes accompanying the transition can be explained by a rigid-body rotation of half of the factor XIII dimers in the lattice by about 5°. The remaining changes are mostly small interdomain movements of the four domains which constitute one factor XIII monomer.

1. Introduction

Factor XIII is the last enzyme in the blood-coagulation cascade. It is a transglutaminase and catalyzes the formation of γ-glutaminyl-ε-lysyl-isopeptide bonds between fibrin molecules, thus stabilizing the fibrin clot. It also crosslinks α_2-antiplasmin onto the fibrin clot, making the clot less susceptible to fibrinolysis by the serine protease plasmin (Muszbek *et al.*, 1996).

Cellular factor XIII zymogen has been crystallized in two different crystal forms (Hilgenfeld *et al.*, 1990; Bishop *et al.*, 1990) and its three-dimensional structure has been solved (Yee *et al.*, 1994, 1995; Weiss *et al.*, 1998). Factor XIII is an α_2 homodimer, with each monomer consisting of four domains. Thrombin-cleaved factor XIII has also been crystallized (Yee *et al.*, 1995) and the observed crystal form was the same as the monoclinic form observed for the zymogen. In both crystal forms, the active site of a factor XIII monomer, which contains the catalytic triad Cys314-His373-Asp396, is completely buried and shielded from the solvent, suggesting that only an inactive form of the molecule has been crystallized. However, based on the occurrence of two unusual non-proline *cis* peptide bonds in the structure, some ideas concerning a model for the activation of the enzyme have been proposed (Weiss *et al.*, 1998).

Even though our monoclinic crystals of factor XIII diffract to at least 1.9 Å resolution at room temperature on a synchrotron source, only a data set approximately 82% complete to 2.1 Å could be assembled from five crystals owing to problems in scaling and merging data sets from different crystals. Consequently, even the highest resolution and the best quality structure available to date (Weiss *et al.*, 1998) contains some areas which are not well defined in the electron density. These are the six N-terminal and the three C-terminal residues of both monomers, residues 37–39 in the loop

connecting the so-called activation peptide (residues 1–37) to domain 1 (residues 38–185) and residues 510–516 in the loop which connects domain 2 (197–503) to domain 3 (residues 517–628) and domain 4 (residues 632–731).

In order to resolve these ambiguous areas in the structure, we have attempted to collect a complete data set from one single crystal to the highest resolution possible. Owing to the radiation sensitivity of the crystals, this requires the establishment of flash-cooling conditions for monoclinic factor XIII crystals. First trials with conventional cryoprotectants were unsuccessful since the crystals deteriorated visibly upon exposure to any cryoprotectant tried. The use of paraffin oil, which has been studied extensively in our laboratory (Riboldi-Tunnicliffe & Hilgenfeld, 1999), also did not preserve the diffraction quality of the crystals. It led to the formation of ice rings even though care was taken to remove all water from the surface of the crystal. Therefore, we tried to soak the crystals in solutions containing increasing amounts of PEG 6000, which was used as a precipitant in the crystallization of factor XIII, hoping that the already present PEG 6000 would be better tolerated by the crystals.

2. Materials and methods

Recombinant cellular FXIII zymogen was crystallized as described in Hilgenfeld *et al.* (1990) and Weiss *et al.* (1998). 2 µl of protein solution at 2–4 mg ml^{-1} were mixed with 2 µl of reservoir solution and equilibrated against 1 ml of reservoir containing 100 m*M* MES pH 6.2–6.4 and 1–2%(*w*/*v*) PEG 6000. Crystals grew to a maximum size of 0.5 mm in each dimension. The crystals belonged to space group $P2_1$, with unit-cell parameters a = 134.59, b = 72.78, c = 101.05 Å, β = 106.08° and two molecules of 731 amino acids each per asymmetric unit. They diffracted X-rays to a resolution of at least 1.9 Å at ambient temperature using synchrotron radiation at beamline X11 at the EMBL outstation (DESY, Hamburg).

For the purpose of flash-cooling the crystals, they were successively transferred to solutions containing increasing amounts of the precipitant PEG 6000. They were carefully removed from the crystallization drop using an X-ray capillary and placed in 1 ml of reservoir solution containing 2%(*w*/*v*) PEG 6000. In time increments of about 15 min, the crystals were transferred to solutions with 2%(*w*/*v*) incremental increases in PEG 6000 to a final concentration of 48%(*w*/*v*) PEG 6000. Every transfer step was monitored under a light microscope to check for damage to the crystals. At PEG 6000 concentrations of 2, 12, 24, 36 and 48%, one crystal was removed from the solution and mounted in an X-ray capillary. A 1° oscillation picture was taken from the crystals in random orientation on a Nonius FR591 rotating-anode generator operated at 40 kV and 100 mA. The crystal was exposed for 1 h and the picture was recorded on a MAR imaging-plate system (30 cm) at a distance of 150 mm. The image was then indexed using the *DENZO* program (Otwinowski, 1993).

A complete data set was collected from a crystal which was kept in a solution containing 36%(*w*/*v*) for a period of about two weeks. The crystal was flash cooled in a nitrogen stream and data were collected at the X11 beamline at the EMBL outstation (DESY, Hamburg). 289 images comprising a total rotation range of 151° were collected on a 30 cm MAR imaging-plate scanner. The data were indexed and processed using *DENZO* (Otwinowski, 1993) and scaled using *SCALEPACK* (Otwinowski, 1993). Intensities were converted to structure factors using the program *TRUNCATE* (French & Wilson, 1978).

Table 1
Crystallographic analysis of monoclinic factor XIII crystals in various PEG concentrations.

No.	PEG 6000 [%(*w*/*v*)]	*a*† (Å)	*b*† (Å)	*c*† (Å)	β† (°)	Volume (Å^3)	Reduction (%)
1	2	135.0	73.0	101.4	106.0	950586	0.0
2	12	134.4	72.2	101.0	106.0	942105	1.9
3	24	133.7	71.6	100.7	106.4	924772	3.7
4	36	140.3	71.1	185.5	107.8	1761843	8.3‡
5	48	139.3	70.4	184.3	107.9	1719891	10.5‡

† All unit-cell dimensions reported are based on one rotation image of 1° only. ‡ Taking the doubling of the unit-cell volume into account.

The structure was then solved by a combination of molecular replacement and calculation of a native Patterson map using the structure of one dimer of coagulation factor XIII (PDB entry 1f13; Weiss *et al.*, 1998) as a starting model. The rotation function, Patterson correlation refinement of the rotation function maxima and translation functions were all computed using the program *X-PLOR* (Brünger *et al.*, 1987).

One round of refinement was performed using *X-PLOR* (Brünger *et al.*, 1987). After correctly orienting and positioning the two dimers, rigid-body minimization was carried out. Firstly, the two complete dimers were defined as rigid bodies, then all four monomers, and finally each monomer was divided up into five pieces, yielding a total of 20 rigid bodies for refinement. Afterwards, positional parameters and thermal factors for each of the 23112 atoms were refined. No non-crystallographic symmetry restraints were used in the refinement and no water molecules were included.

The superposition and structural comparisons between the starting structure and the two dimers were carried out using the program *LSQKAB* (Collaborative Computational Project, Number 4, 1994), which is based on the vector-superposition algorithm developed by Kabsch (1978).

3. Results and discussion

As can be seen from the data presented in Table 1, increasing amounts of PEG 6000 in the soaking solution lead to a concomitant dehydration of the crystal. The relationship is almost linear: addition of roughly 12%(*w*/*v*) PEG 6000 leads to a decrease of the unit-cell volume by about 2%. At a concentration of about 34–36% PEG 6000 a non-linear behaviour was observed. The crystal developed visible cracks even upon very careful transfer. These cracks annealed again after a while, but exposure to X-rays of the crystal revealed that a phase transition had accompanied the appearance of the

Table 2
Data-collection statistics.

Values in parentheses refer to the outermost resolution shell (2.35–2.27 Å).

Number of crystals	1
a (Å)	137.67
b (Å)	69.22
c (Å)	183.20
β (°)	107.27
Resolution limits (Å)	25.0–2.27
Total number of reflections	429995
Unique reflections	150837
Redundancy	2.85
Completeness (%)	99.0 (98.3)
$I/\sigma(I)$	18.9 (5.5)
$R_{\rm merge}$† (%)	4.0 (20.7)
$R_{\rm r.i.m.}$‡ (%)	4.8 (25.8)
$R_{\rm p.i.m.}$§ (%)	2.8 (15.1)

† $R_{\rm merge} = \sum_{hkl}\sum_i |I_i(hkl) - \overline{I(hkl)}| / \sum_{hkl}\sum_i I_i(hkl)$, where $\sum_{hkl}$ denotes the sum over all reflections and $\sum_i$ the sum over all equivalent and symmetry-related reflections (Stout & Jensen, 1968). ‡ $R_{\rm r.i.m.}$ is the redundancy-independent merging R factor (Weiss & Hilgenfeld, 1997), which is identical to the $R_{\rm meas}$ of Diederichs & Karplus (1997). $R_{\rm r.i.m.} = \sum_{hkl}[N/(N-1)]^{1/2}\sum_i |I_i(hkl) - \overline{I(hkl)}| / \sum_{hkl}\sum_i I_i(hkl)$, with N being the number of times a given reflection has been observed. § $R_{\rm p.i.m.}$ is the precision-indicating merging R factor (Weiss & Hilgenfeld, 1997). $R_{\rm p.i.m.} = \sum_{hkl}[1/(N-1)]^{1/2}\sum_i |I_i(hkl) - \overline{I(hkl)}| / \sum_{hkl}\sum_i I_i(hkl)$.

cracks. The unit-cell volume was approximately doubled. Taking that doubling into account, the unit-cell volume decreased by about 5% between 24 and 36% PEG 6000, *i.e.* two and a half times the decrease in other 12% PEG concentration changes.

A crystal soaked in a 36% PEG solution for about two weeks was flash-cooled in a nitrogen stream at the X11 beamline at the EMBL outstation (DESY, Hamburg). The crystal diffracted to about 2.1–2.0 Å resolution as judged by a visual inspection of the first diffraction image. Compared with the form *A* crystals at room temperature, the diffraction power was somewhat diminished. This is in contrast to findings on other crystals, where it has been reported that the resolution limit could even be extended by soaking the crystals in increasing concentrations of the precipitant used (Schick & Jurnak, 1994; Esnouf *et al.*, 1998). The reason for this is probably the strain which our crystal experienced during the phase transition. For practical reasons, it was necessary to limit the highest resolution for data collection to about 2.27 Å. A complete data set was then collected from this one crystal. The data collection and processing statistics are given in Table 2. It is clear from the $I/\sigma(I)$ values that the diffraction extends beyond 2.27 Å, but not much. All the indicators commonly used to assess the quality of X-ray data as well as the novel redundancy-independent merging R factor ($R_{\rm r.i.m.}$) and the precision-indicating merging R factor ($R_{\rm p.i.m.}$; Weiss & Hilgenfeld, 1997) prove that the data set is of very high quality.

The unit-cell dimensions given in Table 2 show that flash-cooling a crystal soaked in a 36% PEG solution for a longer period of time decreased the unit-cell volume even further. From the crystallographic data given in Table 2, a unit-cell volume of 1667100 Å^3 can be calculated, which is about 5.4% smaller than the volume determined from the room-temperature unit-cell dimensions. Even though one has to be cautious in comparing these two numbers because in one case the unit-cell dimensions were determined from only one image of 1° whereas in the other the dimensions were determined from a complete data set with a total rotation range of 151°, a clear trend is discernible in any case.

Comparing the unit-cell parameters with the previously published values of a = 134.59, b = 72.78, c = 101.05 Å, β = 106.08° (Weiss *et al.*, 1998) at room temperature and at 2%(*w*/*v*) PEG 6000, the total reduction in volume is about 12.4%. With a molecular weight for the factor XIII zymogen monomer of 83071 kDa and two molecules per asymmetric unit for the 2% PEG 6000 crystal form at room temperature, the Matthews parameter V_M (Matthews, 1976) is 2.86 Å^3 Da^{-1} and the solvent content 57.0%. For the 36% PEG 6000 crystal form at 100 K, the V_M is 2.51 Å^3 Da^{-1} and the solvent content is 51.0%. Assuming that the protein volume remains constant, the total reduction of volume is taken up by the solvent space. Of the approximately 9000 solvent molecules in the asymmetric unit of the 2% PEG 6000 crystal form at room temperature, about 2000 were expelled from the crystal. For the orthorhombic crystal form of the EF–Tu–Ts complex, Schick & Jurnak (1994) reported a shrinkage of the unit-cell volume by 11.5% upon transfer of a crystal grown at 20%(*w*/*v*) PEG 4000 to a mixture of a low molecular weight and a high molecular weight PEG. Even though visible cracks developed during the transfer, no change of symmetry occurred.

The relationship between the two crystal forms of factor XIII is depicted in Fig. 1. The previously reported form will be called form *A* from now on and the new form with the doubled unit-cell volume form *B*. Interestingly, the space group $P2_1$ is the same in both forms. During the transition from form *A* to form *B* the $(a + c)$ axis of form *A* becomes the *a* axis of form *B*, the *b* axes remain the same in both forms and the $(-a + c)$ axis of form *A* becomes the *c* axis of form B. This means that every second 2_1 screw axis is lost upon the transition (those in red in Fig. 1), whereas the other 50% remain intact crystallographic 2_1 screw axes. This transition requires a highly concerted movement of one-half of the molecules in the crystal. Previous studies on water-mediated transformations in protein crystals date back to at least the late 1940s (Boyes-Watson *et al.*, 1947; Huxley & Kendrew, 1953). They have been ascribed to moving layers of protein molecules. More recently, a systematic study was undertaken by Salunke *et al.* (1985), but most observed transformations only involve a continuous or discontinuous shrinkage of the unit-cell volume without any apparent change in symmetry (Salunke *et al.*, 1985; Schick & Jurnak, 1994; Esnouf *et al.*, 1998). The only exception is the transformation which occurs in monoclinic lysozyme crystals upon dehydration (Salunke *et al.*, 1985). Here, a pseudo-*B*-centered monoclinic cell is transformed into a true *B*-centered cell, which could then be described by a primitive cell with half the original unit-cell volume. As in our case, this requires the concerted movement of half the protein molecules in the crystal lattice.

The structure solution and refinement proceeded in a relatively straightforward manner. From the relationship between the unit cells in the two crystal forms (see Fig. 1), it is

clear that the factor XIII dimer of the starting model (PDB entry 1f13; Weiss *et al.*, 1998) has to be rotated by about 40° about the *b* axis. The exact rotation angles as determined using the program *X-PLOR* (Brünger *et al.*, 1987) were, in Eulerian angles, $(\theta_1, \theta_2, \theta_3) = (335.3, 43.2, 95.3^\circ)$ or $(268.2, 43.2, 88.2^\circ)$, with the two rotations corresponding to the two possible orientations of the twofold symmetric dimers. The second rotation yielded a slightly higher correlation coefficient in the Patterson correlation refinement; this set of angles was therefore used to calculate the translation function. The translation of the two dimers in fractional coordinates were $(x, y, z) = (0.24, 0.0, 0.24)$ and $(0.77, 0.98, 0.76)$. The distance between the two corresponds to the highest non-origin peak of the native Patterson function. After rigid-body refinement at increasing resolution, the *R* factor in the resolution range 10.0–3.0 Å was 34.0% ($R_{\rm free}$ = 33.8%) and after a complete round of refinement which included simulated-annealing and temperature-factor refinement, the *R* factor in the resolution range 25.0–2.27 Å was 24.1% ($R_{\rm free}$ = 30.4%). No non-crystallographic symmetry restraints were used in order to avoid masking any possible differences between the molecules that could have arisen from the phase transition.

A superposition of the two factor XIII dimers in the asymmetric unit of crystal form *B* using the program *LSQKAB* (Kabsch, 1978) based on a total of 1438 C^α positions yielded an r.m.s. difference of 0.50 Å and a rotation angle between the two dimers of 4.8°. This already shows a major effect of the transition. The two dimers that were crystallographically equal in crystal form *A* are now related by a rotation of nearly 5°. The overall r.m.s. differences of the two dimers to the starting structure (PDB entry 1f13; Weiss *et al.*, 1998) are 0.70 and 0.63 Å, respectively, which is only slightly higher than the r.m.s. difference between the two dimers.

A pairwise superposition of the four factor XIII monomers in the asymmetric unit yielded r.m.s. deviations based on 719 C^α positions of 0.37–0.77 Å. The r.m.s. deviations to the two starting monomers are in the same range (0.43–0.76 Å) and the r.m.s. deviation between the two starting monomers is 0.50 Å. A domainwise superposition of the four domains of the four monomers in form *B* yielded the following values: 0.26–0.48 Å for domain 1, 0.22–0.33 Å for domain 2, 0.26–0.64 Å for domain 3 and 0.29–0.37 Å for domain 4. These values are mostly in the range of the overall coordinate error of the structure. This means that the domains of the monomers remain intact and that there are small but significant differences in the relative orientation of the domains in the four factor XIII monomers in the asymmetric unit. These interdomain motions are associated with rotation angles of up to 4.4°. For HIV-1 reverse transcriptase, interdomain motions of up to 12° have been reported to occur when crystals are dehydrated (Esnouf *et al.*, 1998). The authors concluded that these changes may reflect the functionally important flexibility of the enzyme. Even though the interdomain motions in factor XIII are smaller than those in HIV-1 reverse transcriptase, they may still exhibit a similar significance. A more detailed analysis of the differences between the two crystal forms of factor XIII including the differences in the water structure will be presented after the structure has been fully refined.

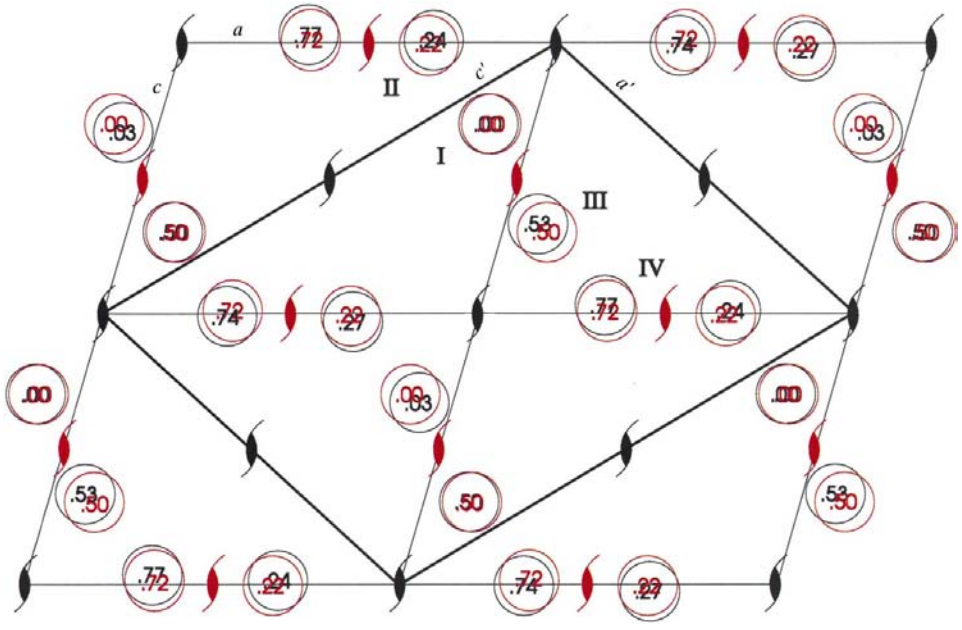

Figure 1
Relationship of the crystal forms *A* (thin lines, red circles, four complete cells shown) and *B* (thick lines, black circles) of factor XIII as shown by a projection of the unit cells onto the respective *ac* planes. The shrinkage of the unit-cell volume upon the transition is neglected in this figure for clarity. The relative (x, z) coordinates of the factor XIII monomers are indicated by the position of the circles; the relative (y) coordinates of the monomers are indicated by the numbers inside the circles.

4. Conclusions

We have observed and described by crystallographic means a phase transition undergone by monoclinic factor XIII crystals upon dehydration. Even though most of the change can be attributed to a rigid-body rotation of the factor XIII dimers in the crystal lattice, small but significant interdomain motions have also been observed. These may provide a clue about the mobility of the four domains of a factor XIII monomer relative to each other in the light of the still not understood activation process.

We would like to thank Dr Hubert J. Metzner (Centeon Pharma, Marburg) for providing pure recombinant factor XIII zymogen for our studies and the crew of the EMBL Outstation (DESY, Hamburg) for their support during data collection.

This work was also supported by the European Bio-Crystallogenesis Initiative (European Commission grant No. BIO4-CT98-0086).

References

Bishop, P. D., Lasser, G. W., Le Trong, I., Stenkamp, R. E. & Teller, D. C. (1990). *J. Biol. Chem.* **265**, 13888–13889.
Boyes-Watson, J., Davidson, E. & Perutz, M. F. (1947). *Proc. R. Soc. London Ser. A*, **191**, 83–132.
Brünger, A. T., Kuriyan, J. & Karplus, M. (1987). *Science*, **235**, 458–460.
Collaborative Computational Project, Number 4 (1994). *Acta Cryst.* D**50**, 760–763.
Diederichs, K. & Karplus, P. A. (1997). *Nature Struct. Biol.* **4**, 269–275.
Esnouf, R. M., Ren, J., Garman, E. F., Somers, D. O'N., Ross, C. K., Jones, E. Y., Stammers, D. K. & Stuart, D. I. (1998). *Acta Cryst.* D**54**, 938–953.
French, G. S. & Wilson, K. S. (1978). *Acta Cryst.* A**34**, 517–525.
Hilgenfeld, R., Liesum, A., Storm, R., Metzner, H. J. & Karges, H. E. (1990). *FEBS Lett.* **265**, 110–112.
Huxley, H. E. & Kendrew, J. C. (1953). *Acta Cryst.* **6**, 76–80.
Kabsch, W. (1978). *Acta Cryst.* A**34**, 827–828.
Matthews, B. W. (1976). *J. Mol. Biol.* **33**, 491–497.
Muszbek, L., Ádány, R. & Mikkola, H. (1996). *Crit. Rev. Clin. Lab. Sci.* **33**, 357–421.
Otwinowski, Z. (1993). *Proceedings of the CCP4 Study Weekend. Data Collection and Processing*, edited by L. Sawyer, N. Isaacs & S. Bailey, pp. 56–62. Warrington: Daresbury Laboratory.
Riboldi-Tunnicliffe, A. & Hilgenfeld, R. (1999). *J. Appl. Cryst.* **32**, 1003–1005.
Salunke, D. M., Veerapandian, B., Kodandapani, R. & Vijayan, M. (1985). *Acta Cryst.* B**41**, 431–436.
Schick, B. & Jurnak, F. (1994). *Acta Cryst.* D**50**, 563–568.
Stout, G. H. & Jensen, L. H. (1968). *X-ray Structure Determination. A Practical Guide*, p. 402. New York: Macmillan.
Weiss, M. S. & Hilgenfeld, R. (1997). *J. Appl. Cryst.* **30**, 203–205.
Weiss, M. S., Metzner, H. J. & Hilgenfeld, R. (1998). *FEBS Lett.* **423**, 291–296.
Yee, V. C., Pedersen, L. C., Bishop, P. D., Stenkamp, R. E. & Teller, D. C. (1995). *Thromb. Res.* **78**, 389–397.
Yee, V. C., Pedersen, L. C., Le Trong, I., Bishop, P. D., Stenkamp, R. E. & Teller, D. C. (1994). *Proc. Natl Acad. Sci. USA*, **91**, 7296–7300.